



Feasibility of Using Cortical Bone as an Ultrasound Reflector to Investigate the Relationship Between Fast and Slow Waves and Porosity: A 2D Simulation Study

Muhamad Amin Abd Wahab^{1,*}, Rubita Sudirman¹, Nasrul Humaimi Mahmood¹, Syarifah Noor Syakiylla Sayed Daud¹, Awais Gul Airij Gul²

¹ Fakulti Kejuruteraan Elektrik, Universiti Teknologi Malaysia, 81310 Skudai, Johor, Malaysia

² Dawood University of Engineering & Technology, Karachi, Pakistan

ARTICLE INFO

Article history:

Received 16 January 2024

Received in revised form 20 September 2024

Accepted 7 October 2024

Available online 20 December 2024

Keywords:

Ultrasound; fast and slow wave;
bandlimited deconvolution; cancellous
bone

ABSTRACT

In the context of the ultrasound pulse-echo (PE) technique, extracting distinct fast and slow waves presents challenges due to their frequent overlap and interference with unwanted scattering waves within cancellous bone. This study aims to explore the viability of utilizing cortical bone as an ultrasound reflector for investigating correlations between fast and slow waves and porosity. Employing a 2-Dimensional (2D) simulation approach, diverse porosity levels within 2D cancellous bone models alongside cortical bone are examined. The bandlimited deconvolution method is applied to isolate fast and slow waves from the original waves. The correlation coefficient is used to compare the result between the original, fast, and slow waves. Results indicate enhanced correlations of fast ($R^2_{\text{fast}} = 0.78$) and slow ($R^2_{\text{slow}} = 0.76$) waves with porosity compared to the original waveform ($R^2_{\text{original}} = 0.45$). Incorporating fast and slow wave analyses could potentially enhance porosity estimation accuracy through the PE ultrasound measurements technique.

1. Introduction

Bone quality checks regularly can be one method of disease prevention for Osteoporosis, cancers, and osteogenesis imperfecta before it gets worse [1, 2]. In addition to x-ray-based methods like quantitative computed tomography (QCT) and dual X-ray absorptiometry (DXA), an ultrasound-based alternative called quantitative ultrasound (QUS) is presented, providing a safer, more cost-effective, and portable solution. The QUS method predicted bone quality by analysing ultrasound waves based on their attenuation and velocity [3]. Previous researchers indicate that the ultrasound fast and slow waves can propagate through cancellous bone and its parameters are associated more with various cancellous bone attributes [4-6]. Generally, the fast wave refers to the waves which correspond to solid trabecular and the slow wave is the waves that correspond to the pore part of cancellous bone

* Corresponding author.

E-mail address: muhamadamin.abdwahab@utm.my

<https://doi.org/10.37934/araset.54.1.176183>

[7]. Analysing these waves via ultrasound technology could enhance bone quality assessment accuracy.

Earlier finite difference time domain (FDTD) simulations have demonstrated the emergence of fast and slow waves in the reflected wave using the PE technique. These findings suggest the potential to enhance the accuracy of bone quality estimation through these techniques by utilizing fast and slow waves [4, 8-11]. Despite that, the method proposed required perfect reproducibility which only can be achieved using a simulation approach [4, 11]. Presently, a definitive technique for extracting fast and slow ultrasound waves via the PE method is lacking. This challenge arises due to the frequent overlap of fast and slow waves, combined with interference from undesired scattering waves within cancellous bone. Additionally, given that a significant portion of the cancellous bone structure is encased by cortical bone, the interface between the cortical and cancellous bone surfaces can be effectively utilized as an ultrasound reflector. Thus, this investigation aims to assess the feasibility of employing cortical bone as an ultrasound reflector to study correlations between fast and slow waves and different porosity levels. Using a 2D simulation approach, diverse porosity variations are examined within 2D cancellous bone models in conjunction with cortical bone. The bandlimited deconvolution method proposed by Wear [12, 13] is utilized to disentangle fast and slow waves from the original wave. The correlation coefficient facilitates a comparative analysis of outcomes among the original, fast, and slow waves. Subsequently, a comparison and discussion of the correlation behaviour with findings from prior research will be presented. This work introduces novel aspects which suggest an alternate method to enhance precision in current PE measurements by incorporating cortical bone as a reflector to the fast and slow waves for bone quality assessment.

2. Materials and Method

2.1 2-Dimensional (2D) Cancellous Models

The 2-D cancellous model is a model of cancellous bone from previous works by Gilbert *et al.*, [5]. There are 9 cancellous models with porosity levels ranging from 30% to 75% used in the simulation. Table 1 shows the acoustic and material properties of bone and water based on the acoustic properties database from the signal-processing website [14].

Table 1

Materials properties for the simulation

No.	Material	Colour label	No. Label	ρ (g/cm ³)	ϕ	v (m/s)
1.	Water	White	1	1000	-	Cl: 1497 Cs: 0
2.	Bone	Black	2	2000	30% -75%	Cl: 3500 Cs: 2400

ϕ : Porosity, ρ : Density, v: Velocity, Cl: Longitudinal Velocity, Cs: Shear Velocity

2.2 2-Dimensional (2D) Simulation Setup for Pulse-Echo Measurement Technique

SimNDT version 0.52 by Molero *et al.*, [15] is the software used for this investigation. The simulation setup was based on the PE measurement technique with a 1 MHz single Gaussian sine wave as the output pulse for the transducer. Referring to Figure 1, the transducer was a planar type with a size of 9 mm. The distance between the transducer and bone models is 7 mm. An absorbing layer with a thickness of 5 mm surrounded the simulation area. The black rectangular structure with a thickness of 1 mm at the top and bottom of the bone models is assumed as a cortical bone. The

blue arrow represents the location of the wave that will be analysed, which is on the front surface of the bottom cortical bone.

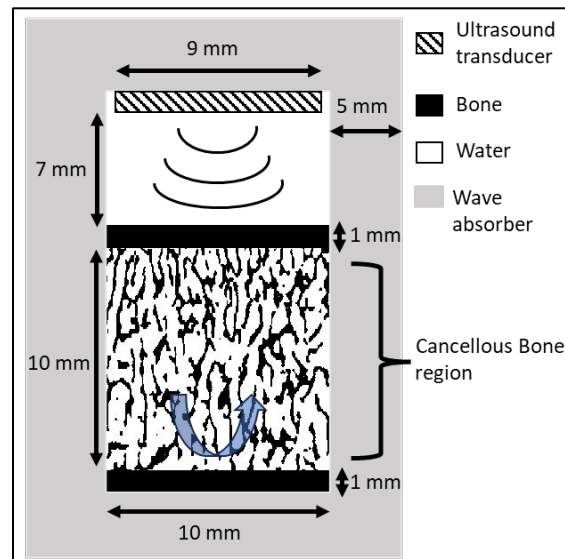


Fig. 1. Simulation setup

The water-only wave, essential for bandlimited deconvolution and ultrasound parameter calculations in this simulation, is generated using the identical setup depicted in Figure 1. However, the cancellous bone region is omitted and replaced solely with water. To precisely determine the arrival time of the targeted reflected wave, a reference simulation is conducted involving the removal of the upper cortical and cancellous bone regions, while retaining the lower cortical bone. The simulation time was set to 30 μ s and the pulse of the input voltage was set to 500 volts peak-to-peak (V_{pp}).

2.3 Bandlimited Deconvolution Method and Ultrasound Parameters

The bandlimited deconvolution method separates the original or mixed (single mode) wave into distinct fast and slow waves [12, 13]. The bandlimited deconvolution method's basis rests on Eq. (1), developed by Marutyan *et al.*, [16] which serves as a mathematical model for ultrasound wave propagation through porous structures.

$$Y(f) = X(f)[H_{fast}(f) + H_{slow}(f)] \quad (1)$$

$X(f)$ represents the spectrum of the wave traversing water alone, and $Y(f)$ denotes the spectrum of the wave traversing a sample (original wave). Here, f stands for ultrasound frequency. The term enclosed within the brackets in Eq. (1) signifies a transmission coefficient. The porous structure's transfer functions, $H_{fast}(f)$ and $H_{slow}(f)$, correspond to two co-propagating waves within a linear frequency-dependent attenuating medium [17]. The bandlimited deconvolution method estimates the transfer function of the fast wave, $h_{fast}(t)$, using the reference wave's velocity exceeding 1479 m/s. As the term suggests, the fast wave is expected to outpace the reference wave. Applying Eq. (1), $h_{fast}(t)$ is calculated through fast fourier transform (FFT) into $h_{fast}(f)$, then multiplied by $X(f)$ to yield $Y_{fast}(f)$. Subsequently, employing inverse FFT (IFFT) on $Y_{fast}(f)$ obtains the fast wave in the time domain, $y_{fast}(t)$. To derive the slow wave in the time domain, $y_{slow}(t)$, the mix wave in the time domain, $y(t)$, is subtracted from $y_{fast}(t)$. Additional details on this methodology are available in

previous studies [12, 18, 19]. The ultrasound parameter involved in this investigation is frequency dependent attenuation (β). The calculation formula for the attenuation parameters is referenced from previous research [12],

$$\beta(f) = \frac{1}{D} [20 \log SB(f) - 20 \log SR(f)] \quad (2)$$

where D is the sample thickness in cm, $SR(f)$ is the amplitude spectrum of a water-only wave and $SB(f)$ is the amplitude spectrum of the bone sample wave. The $\beta(f)$ slope frequency range would be from 0.2 to 0.6 MHz with the unit of dB/cm/MHz.

3. Results and Discussions

Figure 2(a) illustrates the reflected waveform from three distinct simulation setups. In Figure 2(a)(i), a reference simulation (water only, no top cortical or cancellous bone) indicates an arrival time of 23.1 μ s for the reflected waveform F2. This value guides the estimation of F2's arrival times in the water-only and sample cases. Figure 2(a)(ii) displays the estimated waveform received from the water-only simulation, and Figure 2(a)(iii) shows the estimated waveform from a bone sample with 73.52% porosity. The study focuses on the reflected waveform F2.

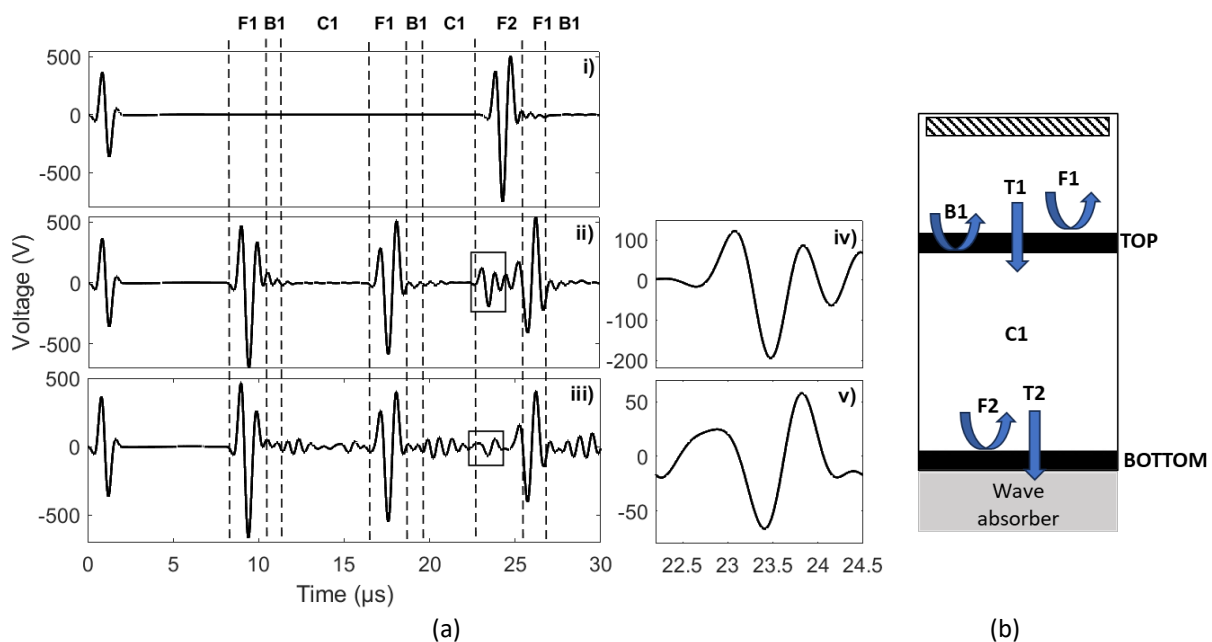


Fig. 2. (a) Example of the reflected waveform received at the receiver and (b) simulation setup diagram for water-only measurement with corresponding reflected waveform from (a)

Figure 2(a) (iv) and (v) magnify Figure 2(a) (ii) and (iii), respectively. F1 and B1 in Figure 2(a) and (b) depict reflected waves at the front and back of the top cortical bone surface. These waves result from back-and-forth reflection between the ultrasound transducer and the top cortical bone surface. Briefly, upon propagating through the top cortical bone, some of the waves are reflected (F1 and B1), refracted and the rest passing through (T1) the cortical bone. As T1 reaches the front of the bottom cortical bone surface, it generates scatter wave C1, which disperses in various directions (reflected, refracted, through); this phenomenon is exclusive to bone samples. Subsequently, weakened wave T1 encounters the front of the bottom cortical bone surface, generating reflected waveform F2, which reflected and returns to the receiver. However, some of the incident waveform (T2) continues

passing through the bottom cortical bone. As the simulation setup is enclosed by an absorbing layer, T2's waveform is absorbed and remains unrecorded by the receiver.

Figure 3(a) depicts an example of fast and slow waves extracted from the reflected waveform F2 (original wave) via the band-limited deconvolution method. Further details regarding the band-limited deconvolution method can be found in previous research [12]. The fast wave exhibits a slightly lower amplitude in comparison to the slow wave, and notably, it arrives ahead or at an earlier time than the slow wave. The findings align well with prior research, indicating that fast waves typically exhibit lower amplitudes and frequently arrive earlier than slow waves [4, 6, 20-23]. The lower amplitude is indication of experiencing higher attenuation effect. The lower amplitude signifies an increase in attenuation effect. As illustrated in Figure 3(b), the average frequency is 0.94 MHz for fast waves and 1.1 MHz for slow waves. Earlier studies have noted the swifter attenuation of high-frequency ultrasound waves compared to low-frequency signals [22, 24]. The fast wave undergoes a more obvious attenuation effect in comparison to the slow wave, resulting in the attenuation of its high-frequency component and the predominance of its lower frequency component upon reaching the receiver.

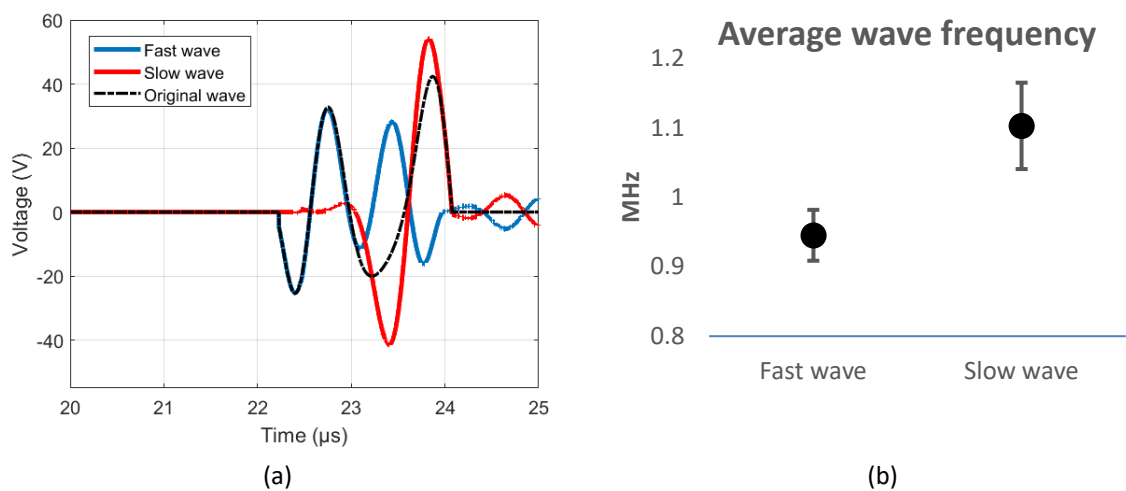


Fig. 3. (a) Example of original, fast, and slow wave for the cancellous bone sample with porosity of 66.5 %. (b) The average frequency content for fast and slow wave

In Figure 4(a) and (b), the original and fast wave attenuation trends exhibit parabolic behaviour with polynomial R^2 values of 0.45 and 0.77, respectively. Meanwhile, the slow wave's attenuation demonstrates a decreasing trend with an R^2 value of 0.76. The attenuation effect for the slow wave diminishes as porosity increases. Higher porosity reduces solid structure compactness, increasing distances between pore spaces. This alteration enhances fluid flow [25], thereby boosting the effectiveness of slow wave propagation and reducing attenuation. This alignment with prior research links the slow wave to cancellous bone pore characteristics [9, 21, 26-28].

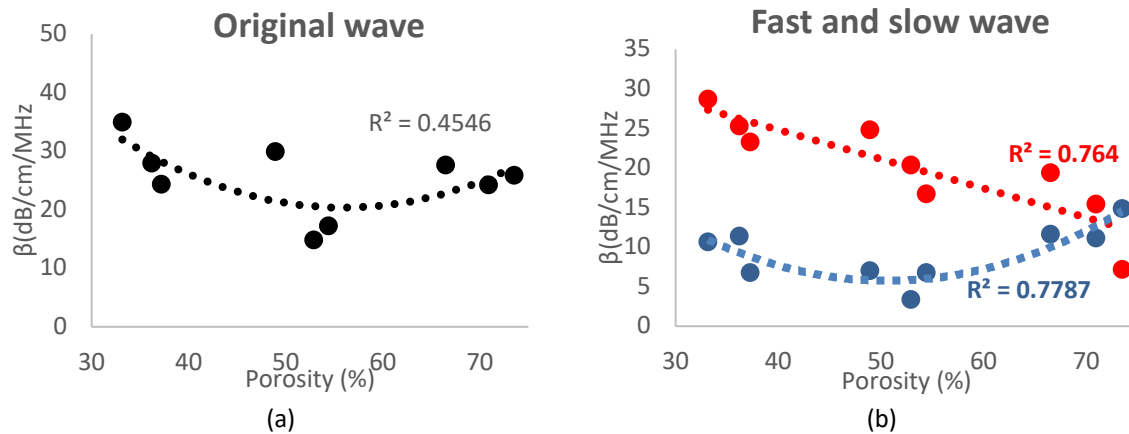


Fig. 4. Ultrasound attenuation parameters versus porosity. (a) Original wave and (b) slow (blue) and fast (red) wave

At high porosity levels, the attenuation of fast and slow waves approaches the same convergence region. This phenomenon is consistent with prior findings, where the attenuation of the fast wave converges with the slow wave's value at 90% porosity (high porosity). Slow wave attenuation predominantly dominates various frequency ranges, particularly in high-porosity cancellous bone [22]. In this study, since the behaviour of the original and fast wave is almost identical, the original wave seems to be dominated by the fast wave. Furthermore, marginally higher fast wave attenuation in low porosity samples might stem from heightened structural compactness-associated attenuation. At mid porosity values, the ample space within the solid structure enables efficient wave propagation; the compatibility between the fast wave and solid structure contributes to the low attenuation. Nonetheless, in high porosity samples, the scarcity of solid structures for fast wave propagation elevates attenuation. Additionally, scattering effects due to trabecular structure inhomogeneity [29, 30] in high porosity bone models could contribute to overall fast wave attenuation, thus explaining its increasing trend. However, the behaviour of fast and slow waves requires more clarity through extensive data and accurate 3D simulations. Also, real bone structures might yield varied results due to non-flat boundaries between cortical and cancellous bone. While the paper showcases the feasibility of using flat cortical bone surfaces as ultrasound reflectors for PE measurements, these limitations suggest areas for future research.

4. Conclusions

The bandlimited deconvolution approach effectively separates and estimates the reflected fast and slow waves from the mixed wave obtained via the PE measurement technique. By analyzing center frequency and attenuation, these waves are discerned and predicted, characterizing their passage through solid and pore regions. Fast waves traverse solid structures, while slow waves navigate the porous regions. The comprehensive simulation results indicate substantial correlation coefficients between the reflected fast and slow wave parameters and porosity, surpassing those of the original wave. These collective findings suggest that incorporating fast and slow waves for bone quality estimation presents a viable alternative, potentially enhancing the accuracy of PE measurements.

Acknowledgement

This work was financially supported by the Universiti Teknologi Malaysia under the University Encouragement Grant Q.J130000.3823.31J55.

References

- [1] Ismail, Rifky, Deni Fajar Fitriyana, Athanasius Priharyoto Bayuseno, Rafi Munanda, Rilo Chandra Muhamadin, Fariz Wisda Nugraha, Andri Setiyawan et al. "Design, manufacturing and characterization of biodegradable bone screw from PLA prepared by Fused Deposition Modelling (FDM) 3D printing technique." *Journal of Advanced Research in Fluid Mechanics and Thermal Sciences* 103, no. 2 (2023): 205-215. <https://doi.org/10.37934/arfmts.103.2.205215>
- [2] LeBoff, Meryl S., S. L. Greenspan, K. L. Insogna, E. M. Lewiecki, K. G. Saag, A. J. Singer, and E. S. Siris. "The clinician's guide to prevention and treatment of osteoporosis." *Osteoporosis international* 33, no. 10 (2022): 2049-2102. <https://doi.org/10.1007/s00198-021-05900-y>
- [3] Laugier, Pascal. *Bone quantitative ultrasound*. Edited by Guillaume Häät. Vol. 576. Dordrecht: Springer, 2011. <https://doi.org/10.1007/978-94-007-0017-8>
- [4] Hosokawa, Atsushi. "Numerical analysis of ultrasound backscattered waves in cancellous bone using a finite-difference time-domain method: isolation of the backscattered waves from various ranges of bone depths." *IEEE transactions on ultrasonics, ferroelectrics, and frequency control* 62, no. 6 (2015): 1201-1210. <https://doi.org/10.1109/TUFFC.2014.006946>
- [5] Gilbert, Robert P., Philippe Guyenne, and Jing Li. "Numerical investigation of ultrasonic attenuation through 2D trabecular bone structures reconstructed from CT scans and random realizations." *Computers in biology and medicine* 45 (2014): 143-156. <https://doi.org/10.1016/j.compbiomed.2013.12.005>
- [6] Kawasaki, Satoshi, Ryohei Ueda, Akihiko Hasegawa, Akifumi Fujita, Teruhisa Mihata, Mami Matsukawa, and Masashi Neo. "Ultrasonic wave properties of human bone marrow in the femur and tibia." *The Journal of the Acoustical Society of America* 138, no. 1 (2015): EL83-EL87. <https://doi.org/10.1121/1.4922764>
- [7] Groopman, Amber M., Jonathan I. Katz, Mark R. Holland, Fuminori Fujita, Mami Matsukawa, Katsunori Mizuno, Keith A. Wear, and James G. Miller. "Conventional, Bayesian, and Modified Prony's methods for characterizing fast and slow waves in equine cancellous bone." *The Journal of the Acoustical Society of America* 138, no. 2 (2015): 594-604. <https://doi.org/10.1121/1.4923366>
- [8] Hosokawa, Atsushi. "Numerical analysis of fast and slow waves backscattered from various depths in cancellous bone." In *2015 IEEE International Ultrasonics Symposium (IUS)*, pp. 1-4. IEEE, 2015. <https://doi.org/10.1109/ULTSYM.2015.0511>
- [9] Hosokawa, Atsushi. "Variations in reflection properties of fast and slow longitudinal waves in cancellous bone with boundary condition." In *2013 IEEE International Ultrasonics Symposium (IUS)*, pp. 2076-2079. IEEE, 2013. <https://doi.org/10.1109/ULTSYM.2013.0530>
- [10] Hosokawa, Atsushi. "Numerical investigation of reflection properties of fast and slow longitudinal waves in cancellous bone: Variations with boundary medium." *Japanese Journal of Applied Physics* 53, no. 7S (2014): 07KF13. <https://doi.org/10.7567/JJAP.53.07KF13>
- [11] Hosokawa, Atsushi. "Numerical analysis of backscatter properties of fast and slow waves in cancellous bone." *Japanese Journal of Applied Physics* 59, no. 3 (2020): 036504. <https://doi.org/10.35848/1347-4065/ab7720>
- [12] Wear, Keith A. "Time-domain separation of interfering waves in cancellous bone using bandlimited deconvolution: Simulation and phantom study." *The Journal of the Acoustical Society of America* 135, no. 4 (2014): 2102-2112. <https://doi.org/10.1121/1.4868473>
- [13] Wear, Keith, Yoshiki Nagatani, Katsunori Mizuno, and Mami Matsukawa. "Fast and slow wave detection in bovine cancellous bone in vitro using bandlimited deconvolution and Prony's method." *The Journal of the Acoustical Society of America* 136, no. 4 (2014): 2015-2024. <https://doi.org/10.1121/1.4895668>
- [14] Signal-Processing. *Ultrasonic or ultrasound sound velocity and impedance*.
- [15] Molero-Armenta, Miguel, Ursula Iturrarán-Viveros, Sofía Aparicio, and Margarita González Hernández. "Optimized OpenCL implementation of the elastodynamic finite integration technique for viscoelastic media." *Computer Physics Communications* 185, no. 10 (2014): 2683-2696. <https://doi.org/10.1016/j.cpc.2014.05.016>
- [16] Marutyan, Karen R., G. Larry Bretthorst, and James G. Miller. "Bayesian estimation of the underlying bone properties from mixed fast and slow mode ultrasonic signals." *The Journal of the Acoustical Society of America* 121, no. 1 (2007): EL8-EL15. <https://doi.org/10.1121/1.2401198>
- [17] Marutyan, Karen R., Mark R. Holland, and James G. Miller. "Anomalous negative dispersion in bone can result from the interference of fast and slow waves." *The Journal of the Acoustical Society of America* 120, no. 5 (2006): EL55-EL61. <https://doi.org/10.1121/1.2357187>
- [18] Abd Wahab, Muhamad Amin, Rubita Sudirman, Mohd Azhar Abdul Razak, Fauzan Khairi Che Harun, and Nurul Ashikin Abdul Kadir. "Comparison of fast and slow wave correlation with various porosities between two measurement technique." In *2019 IEEE Student Conference on Research and Development (SCORED)*, pp. 39-44. IEEE, 2019. <https://doi.org/10.1109/SCORED.2019.8896305>

- [19] Abd Wahab, Muhamad Amin, Rubita Sudirman, Mohd Azhar Abdul Razak, Fauzan Khairi Che Harun, Nurul Ashikin Abdul Kadir, and Nasrul Humaimi Mahmood. "Incident and reflected two waves correlation with cancellous bone structure." *TELKOMNIKA (Telecommunication Computing Electronics and Control)* 18, no. 4 (2020): 1968-1975. <https://doi.org/10.12928/telkomnika.v18i4.14828>
- [20] Nagatani, Yoshiki, Vu-Hieu Nguyen, Salah Naili, and Guillaume Haïat. "The effect of viscoelastic absorption on the fast and slow wave modes in cancellous bone." In *2015 6th European Symposium on Ultrasonic Characterization of Bone*, pp. 1-2. IEEE, 2015. <https://doi.org/10.1109/ESUCB.2015.7169902>
- [21] Otani, Takahiko. "Quantitative estimation of bone density and bone quality using acoustic parameters of cancellous bone for fast and slow waves." *Japanese journal of applied physics* 44, no. 6S (2005): 4578. <https://doi.org/10.1143/JJAP.44.4578>
- [22] Cardoso, Luis, Frédéric Teboul, Laurent Sedel, Christian Oddou, and Alain Meunier. "In vitro acoustic waves propagation in human and bovine cancellous bone." *Journal of Bone and Mineral Research* 18, no. 10 (2003): 1803-1812. <https://doi.org/10.1359/jbmr.2003.18.10.1803>
- [23] Nelson, Amber M., Joseph J. Hoffman, Mark R. Holland, and James G. Miller. "Single mode analysis appears to overestimate the attenuation of human calcaneal bone based on Bayesian-derived fast and slow wave mode analysis." In *2012 IEEE International Ultrasonics Symposium*, pp. 1015-1018. IEEE, 2012. <https://doi.org/10.1109/ULTSYM.2012.0254>
- [24] Wear, Keith A. "Ultrasonic scattering from cancellous bone: a review." *IEEE transactions on ultrasonics, ferroelectrics, and frequency control* 55, no. 7 (2008): 1432-1441. <https://doi.org/10.1109/TUFFC.2008.818>
- [25] Lee, Kang Il. "Relationships of linear and nonlinear ultrasound parameters with porosity and trabecular spacing in trabecular-bone-mimicking phantoms." *The Journal of the Acoustical Society of America* 140, no. 6 (2016): EL528-EL533. <https://doi.org/10.1121/1.4972530>
- [26] Hosokawa, Atsushi, Yoshiki Nagatani, and Mami Matsukawa. "The fast and slow wave propagation in cancellous bone: Experiments and simulations." *Bone Quantitative Ultrasound* (2011): 291-318. https://doi.org/10.1007/978-94-007-0017-8_11
- [27] Mézière, Fabien, Marie Muller, Emmanuel Bossy, and Arnaud Derode. "Measurements of ultrasound velocity and attenuation in numerical anisotropic porous media compared to Biot's and multiple scattering models." *Ultrasonics* 54, no. 5 (2014): 1146-1154. <https://doi.org/10.1016/j.ultras.2013.09.013>
- [28] Hoffman, Joseph J., Amber M. Nelson, Mark R. Holland, and James G. Miller. "Cancellous bone fast and slow waves obtained with Bayesian probability theory correlate with porosity from computed tomography." *The Journal of the Acoustical Society of America* 132, no. 3 (2012): 1830-1837. <https://doi.org/10.1121/1.4739455>
- [29] Pakula, Michal. "On the modeling of wave propagation in cancellous bone." In *2015 6th European Symposium on Ultrasonic Characterization of Bone*, pp. 1-4. IEEE, 2015. <https://doi.org/10.1109/ESUCB.2015.7169906>
- [30] Abderrazek, Bennamane, and Boutkedjirt Tarek. "Ultrasonic non-destructive characterization of trabecular bone: Experimental and theoretical prediction of the ultrasonic attenuation." In *2015 3rd International Conference on Control, Engineering & Information Technology (CEIT)*, pp. 1-6. IEEE, 2015. <https://doi.org/10.1109/CEIT.2015.7233056>